6696 *Biochemistry* **2010,** *49,* 6696–6704
DOI: 10.1021/bi100798w

BIOCHEMISTRY
including biophysical chemistry & molecular biology
Article

Attractant and Repellent Signaling Conformers of Sensory Rhodopsin−Transducer Complexes[†]

Oleg A. Sineshchekov, Jun Sasaki, Jihong Wang, and John L. Spudich*

Center for Membrane Biology, Department of Biochemistry and Molecular Biology, University of Texas Medical School, Houston, Texas 77030

Received May 19, 2010; Revised Manuscript Received June 29, 2010

ABSTRACT: Attractant and repellent signaling conformers of the dual-signaling phototaxis receptor sensory rhodopsin I and its transducer subunit (SRI−HtrI) have recently been distinguished experimentally by the opposite connection of their retinylidene protonated Schiff bases to the outwardly located periplasmic side and inwardly located cytoplasmic side. Here we show that the pK_a of the outwardly located Asp76 counterion in the outwardly connected conformer is lowered by ∼1.5 units from that of the inwardly connected conformer. The pK_a difference enables quantitative determination of the relative amounts of the two conformers in wild-type cells and behavioral mutants prior to photoexcitation, comparison of their absorption spectra, and determination of their relative signaling efficiency. We have shown that the one-photon excitation of the SRI−HtrI attractant conformer causes a Schiff base connectivity switch from inwardly connected to outwardly connected states in the attractant signaling photoreaction. Conversely, a second near-UV photon drives the complex back to the inwardly connected conformer in the repellent signaling photoreaction. The results suggest a model of the color-discriminating dual-signaling mechanism in which phototaxis responses (his-kinase modulation) result from the photointerconversion of the two oppositely connected SRI−HtrI conformers by one-photon and two-photon activation. Furthermore, we find that the related repellent phototaxis SRII−HtrII receptor complex has an outwardly connected retinylidene Schiff base like the repellent signaling forms of the SRI−HtrI complex, indicating the general applicability of macro conformational changes, which can be detected by the connectivity switch, to phototaxis signaling by sensory rhodopsin−transducer complexes.

Many microorganisms use photoreceptors to modulate their motility to seek or avoid regions of illumination depending on light intensity and color. In halophilic archaea, visual pigment-like photoreceptors, sensory rhodopsins, mediate attractant and repellent phototaxis responses by controlling through transducer proteins a his-kinase that modulates the swimming behavior of the cell (*1*−*3*). Sensory rhodopsin I (SRI)[1] is of special interest because it mediates opposite behavior depending on light color: attractant responses (due to transient his-kinase inhibition) upon absorption of a long-wavelength photon and repellent responses (due to transient his-kinase activation) when a second short-wavelength photon is absorbed (*4*). Single mutations have been found in SRI and also in the second subunit of the receptor−transducer complex, the transducer HtrI, which invert the sign of the single-photon response to repellent, and second-site (suppressor) mutations in both subunits cancel the effect of inverter mutations restoring wild-type behavior (*5*−*7*).

We developed an electrophysiological method for measuring the vectoriality and kinetics of light-induced charge movements within rhodopsin molecules in suspensions of *Escherichia coli* cells expressing various microbial rhodopsins (*8*). Using this method, we found that the SRI−HtrI complex exists in two conformational states with opposite connectivity of the retinylidene Schiff base in the photoactive site (*9*). By connectivity of the Schiff base, we mean the direction, inward toward the cytoplasm or outward toward the extracellular medium, of proton release following single-photon absorption. In the conformation that mediates attractant photoresponses, the Schiff base deprotonates toward the cytoplasmic side of the membrane to the inner, cytoplasmic half-channel of SRI. In the repellent-mediating conformation of the complex, the proton is transferred in the opposite direction to the acceptor Asp76 localized in the extracellular half-channel. It should be emphasized that the light-induced proton transfer to Asp76 itself does not play a significant functional role in signaling and reflects only the outwardly connected state of the complex, since the repellent receptor conformer of SRI_D76N−HtrI_E56Q mediates repellent responses and does not deprotonate the Schiff base. Inversion of Schiff base connectivity during the photocycle (often called the connectivity or accessibility switch) is the key event enabling vectorial proton transport and light energy conversion by light-driven proton pumps such as bacteriorhodopsin (*10*). Our data

[†]This work was supported by National Institutes of Health Grant R37GM27750, U.S. Department of Energy Grant DE-FG02-07ER15867, and the Robert A. Welch Foundation.

*To whom correspondence should be addressed. Phone: (713) 500-5473. Fax: (713) 500-0545. E-mail: John.L.Spudich@uth.tmc.edu.

[1]Abbreviations: SRI and SRII, retinylidene phototaxis receptor sensory rhodopsin I and II, respectively; HtrI and HtrII, haloarchaeal taxis transducers that form complexes with SRI and SRII, respectively; Asp76, aspartyl residue at position 76 in SRI. Mutated proteins are identified as follows. SRI_D76N designates an SRI mutant with Asp76 substituted with an asparagine residue. HtrI_E56Q designates an HtrI mutant with the glutamic acid residue at position 56 substituted with glutamine. SRI_D76N−HtrI_E56Q designates the corresponding double mutant of the SRI−HtrI complex.

 Published on Web 06/30/2010

show that this feature of energy-converting microbial rhodopsins is crucial for the sensory pigments as well.

Our electrical data revealed that both conformers are present in the wild-type SRI−HtrI complex, as well as in the inverted (single mutant) and restored (double mutant) complexes (*9*). However, in the wild-type and restored complexes, both of which mediate attractant responses, the conformer equilibrium is poised strongly in favor of that with an inwardly accessible Schiff base. Signal-inverting mutations shift the equilibrium in favor of the outwardly accessible Schiff base form. The amplitude of charge movement depends on two parameters unknown for SRI: the distance over which the Schiff base proton is displaced and the angle between the direction of its movement and the membrane. Therefore, the electrical data do not allow quantitative determination of the relative sizes of the attractant and repellent conformer pools in the wild-type and mutated complexes.

To test for the existence of the two conformer pools by another method and also to enable quantization of the two pools, we applied absorption spectroscopy of *E. coli* and native *Halobacterium salinarum* membranes containing wild-type (attractant), inverted mutant (repellent), and restored (double mutant attractant) SRI−HtrI complexes. This characterization confirms and extends our understanding of the conformer equilibrium and its role in signaling and, moreover, led us to a mechanistic model of SRI−HtrI complex color-discriminating signaling presented here. Predictions from this model regarding Schiff base connectivity switching in the one-photon and two-photon signaling process in the SRI−HtrI complex and the one-photon SRII−HtrII complex are tested and confirmed by electrical measurements. The data provide compelling evidence of the general applicability of the model to phototaxis signaling by SR−Htr complexes.

MATERIALS AND METHODS

Mutagenesis and Expression. Genes encoding SRI−HtrI fusion proteins, in which the C-terminus of SRI is joined through a flexible linker peptide (ASASNGASA) to the N-terminus of HtrI truncated at position 147, were cloned into expression vector pET-21d (Novagen, Merck KgaA, Darmstadt, Germany) under the control of the T7 promoter between NcoI and BamHI sites. The gene encoding the SRII−HtrII fusion protein, in which the C-terminus of NpSRII (SRII from *Natronomonas pharaonis*) is joined through the same flexible linker peptide to the N-terminus of NpHtrII truncated at position 157, was cloned into pET-21d between NcoI and HindIII. Residue replacement mutations were made using the QuickChange site-directed mutagenesis kits (Stratagene, La Jolla, CA). Expression of the genes in BL21(DE3) was induced by the addition of 1 mM isopropyl β-D-thiogalactopyranoside and 5 μM all-*trans*-retinal.

Genes encoding SRI joined through the same linker peptide to the N-terminus of full-length HtrI were cloned into a halobacterial expression vector under the control of the *bop* promoter as described previously (*11*) between NcoI and XbaI sites. Mutations were introduced by the two-step mega-primer polymerase chain reaction (PCR) method (*12*) with pfu turbo polymerase (Stratagene) or Phusion polymerase (Finzyme, Espoo, Finland). *H. salinarum* strain Pho81Wr$^-$ (BR$^-$HR$^-$SRI$^-$HtrI$^-$SRII$^-$HtrII$^-$, carotenoid-deficient and restriction-deficient) (*12*) was used as the recipient in plasmid transformations. The transformed *H. salinarum* cells were grown to early stationary phase in complex medium containing 1 mg/mL mevinolin as described previously (*7*).

Membrane Preparation. *E. coli* cells expressing SRI−$HtrI_{147}$ suspended in 4 M NaCl and 25 mM MES (pH 6.0) were disrupted by a microfluidizer (Microfluidics, Newton, MA). *H. salinarum* cells expressing SRI−HtrI were disrupted by sonication. Unbroken cells and cell debris were pelleted by low-speed centrifugation (Sorvall RC6 *plus*, Thermo Fisher Scientific Inc., Asheville, NC). The membrane fraction in the supernatant was then pelleted for 1 h at 147000*g* in a Beckman OptimaTM L-100 XP ultracentrifuge (Beckman Coulter Inc., Brea, CA) and suspended in 4 M NaCl and 25 mM MES (pH 6.0).

Absorption Spectroscopy. Absorption spectra in the UV−visible range were recorded on a Cary 4000 spectrophotometer (Varian, Palo Alto, CA) with an integrating sphere. Control absorption spectra of membranes not expressing receptor−transducer complexes were subtracted from those with expression. Optical densities at 850 nm, reflecting mostly light scattering and proportional to membrane concentration, were set equal in experimental and control samples. Residual scattering effects in corrected spectra of the complexes were eliminated (if necessary) by subtraction of a logarithmic-scale linear function based on the slope of optical density between 750 and 850 nm, where no significant absorption of membrane components exists. Titration of absorption changes was conducted with the same samples by an increase in pH in small steps by addition of microliter amounts of non-neutralized 0.5 M Tris buffer (pH 10) and in later steps by 1 M NaOH. The pH of the sample was measured before and after spectral scans, and in cases of minor differences, the averaged value of the pH was used for plotting the titration curves.

Electrical Measurements. Intramolecular charge movements were measured in suspensions of *E. coli* cells expressing the indicated proteins by the method described previously (*8*). The suspension of *E. coli* cells was flashed along the line between two platinum electrodes by a Vibrant HE 355II Tunable Laser (OPOTEK Inc., Carlsbad, CA) set at desired wavelengths. A macroscopic electrical current in the cuvette appeared due to asymmetric absorption of light by each bacterial cell. The electrode remote from the light source was fed into a model 428 low-noise current amplifier (Keithley) with a 2 μs rise time. The signals were digitized and stored using DIGIDATA 1325A and pCLAMP 9.0 (both from Axon Instruments). Flash intensities were attenuated to be below the saturation of the signals. Twenty to 50 signals in 10 s intervals with a maximum sampling rate of 2 μs/point were averaged. If not otherwise indicated, the measuring buffer contained 5 mM Tris-HCl, 1.5 mM NaCl, 0.15 mM $CaCl_2$, and 0.15 mM $MgSO_4$ (pH 7.6).

Cell Motility Measurements. Transformed *H. salinarum* cells were grown in complex medium containing 1 mg/mL mevinolin as described previously (*7*). Cultures at the end of their exponential growth phase were diluted 1:10 in fresh CM and incubated for 1 h at 37 °C with agitation. For motility defined as being in the dark, cell trajectories in nonactinic light at wavelengths of > 720 nm were captured as real-time AVI files using a Flashbus Spectrim Lite Video Capture PCI Card on a Dell Dimension 8300 personal computer running VirtualDub 1.6.19.0 (http://www.virtualdub.org), AVI encoder software for video capture. VirtualDub was set to record 10 frames per second during 30 s of cell swimming. Means of spontaneous reversals of the cells in the dark were measured by tracking each cell captured in the AVI files for 30 s to count the number of reversals. Means and standard deviations were calculated from 20−30 cells.

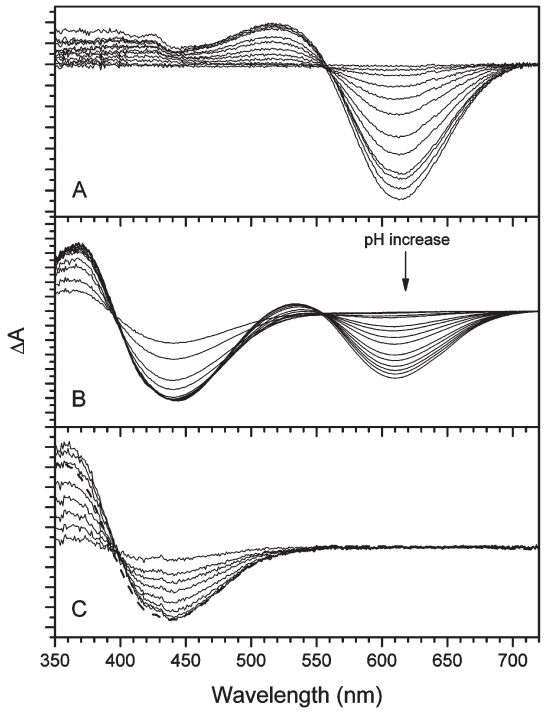

FIGURE 1: pH shift-induced absorption difference spectra in membranes from *H. salinarum* (A) and *E. coli* (B) expressing the wild-type SRI−HtrI complex and membranes from *E. coli* expressing nonfunctional misfolded bacteriorhodopsin (C). The dashed line in panel C is the pH shift-induced difference spectrum for *E. coli* expressing another nonfunctional microbial rhodopsin, an SRI-like pigment from *Salinibacter ruber*. The pH was changed between ~5.5 and ~10 units.

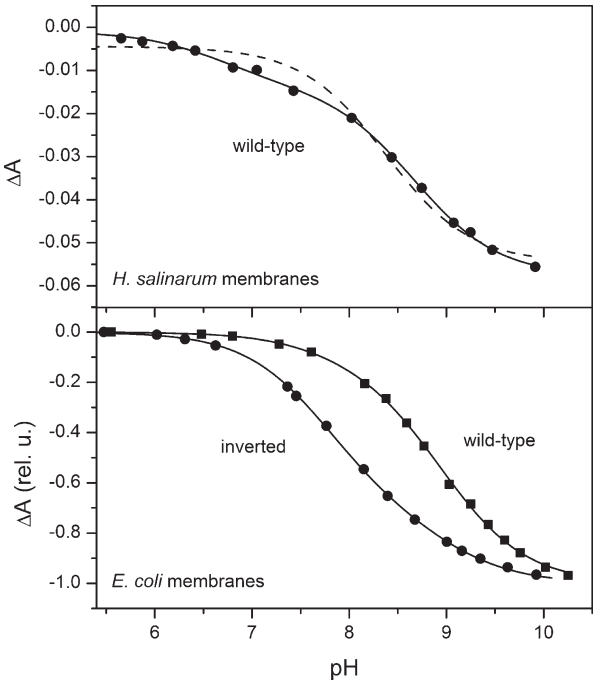

FIGURE 2: Titration of mean absorption changes between 610 and 650 nm. The top panel shows data for the wild-type SRI−HtrI complex in *H. salinarum* membranes. The data were fit with a single component (---) or the sum of two independent components (—). The bottom panel shows titration of absorption changes at 610−650 nm in *E. coli* membranes in 4 M NaCl in wild-type (■) and inverted SRI−HtrI_E56Q (●) complexes. The data were fit with the sum of two independent components.

RESULTS

The Attractant and Repellent Conformers of the SRI−HtrI Complex Differ in Their pK_a Values of the Schiff Base Counterion. The pH titration of the SRI−HtrI complex in *H. salinarum* membranes (Figure 1A) shows difference spectra characteristic of the well-established shift of the absorption maximum from 587 to 552 nm due to deprotonation of the Schiff base counterion Asp76 (*1*). This deprotonation gives rise to absorption difference spectra with a minimum at ~610 nm, a smaller maximum at ~520 nm, and an isosbestic point at 560 nm. However, for the SRI−HtrI complex in *E. coli* membranes, in addition to these long-wavelength bands, a second pH-induced absorption change is observed with a minimum at ~440 nm, a maximum at ~365 nm, and an isosbestic point at 400 nm (Figure 1B).

The short-wavelength titration bands in *E. coli* membranes (Figure 1B) are very similar to the titration bands of misfolded microbial rhodopsins [e.g., bacteriorhodopsin and a eubacterial sensory rhodopsin-like protein (Figure 1C) and *Chlamydomonas* sensory rhodopsin B (also known as channel rhodopsin-2)], which are expressed at high concentrations according to immunoblots yet produce no light-induced charge movements. These bands are most likely due to deprotonation of the retinylidene Schiff base in the misfolded protein, as observed for model retinylidene Schiff base compounds (*1*). We commonly observe variable amounts of spectrally similar misfolded fractions in many other microbial rhodopsins. For our purposes here, it is important to carefully monitor and avoid the contribution of the misfolded protein effect to titrate accurately the Asp76 counterion of SRI in *E. coli* membranes. At low to neutral pH, the superposition of signals due to the functional and misfolded SRI−HtrI complexes leads to suppression of the positive absorption band of the former and shifts its apparent position to a longer wavelength (Figure 1A,B). On the other hand, negligible absorption changes occur at wavelengths above 600 nm in the misfolded proteins (Figure 1C). Therefore, the absorbance changes in the long-wavelength region of the difference spectra (between 610 and 650 nm) were chosen as a measure of the transitions between acid and alkaline forms of SRI. In addition, special attention was paid to exclude other possible distortions of the titration data by processes other than protonation and deprotonation of the Asp76 counterion. Deprotonation of the Schiff base at extremely high pH values was also analyzed, and its perturbing effects were excluded.

A titration curve of wild-type SRI−HtrI complex in native halobacterial membranes obtained with these precautions is fit poorly with a single pK_a, whereas the sum of two independent functions $[A_1/(1 + 10^{x-pK_1}) + A_2/(1 + 10^{x-pK_2})]$ fits well (Figure 2, top). The pK_a values of the two components differ by almost 2 units (~7.0 and 8.8), and the relative amplitude of the low-pK_a component is 20−24%, which matches our earlier published observations (*11*).

We compared the titration of the wild-type complex, which mediates an attractant single-photon response, to that of the SRI−HtrI_E56Q complex, an inverted mutant that produces a strong repellent single-photon response. This mutation is of special interest because it demonstrates that the complex undergoes concerted structural changes since the Glu56 residue in the transducer has a long-distance effect on the photoreaction center in SRI (*9*).

Initially, we investigated both complexes in *E. coli* membranes at 4 M NaCl because of the higher level of expression and stability

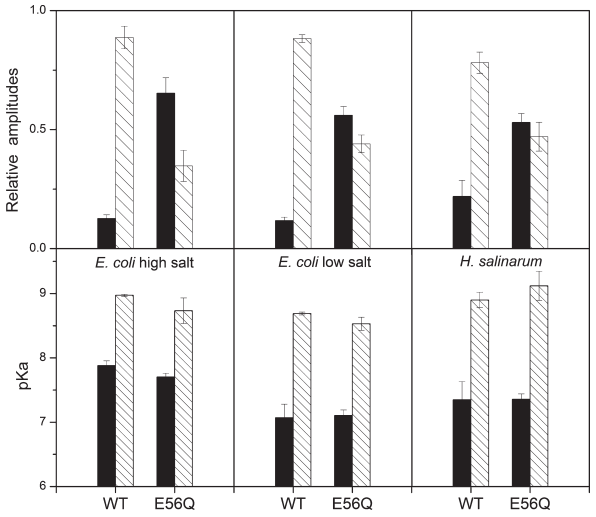

FIGURE 3: Two pK_a values (bottom panels) and corresponding amplitudes of the spectral changes corresponding to each pK_a (top panels), obtained from fitting of the absorption difference spectra of wild-type complexes (first pair of columns in each panel) and inverted SRI−HtrI_E56Q (second pair of columns in each panel) in three types of membrane samples: *E. coli* membranes in 4 M NaCl (left), *E. coli* membranes in 0.1 mM NaCl (middle), and *H. salinarum* membranes (right). Black columns show lower-pK_a components, and striped columns show higher-pK_a components. Error bars represent the errors of fitting the data with the sum of two independent components via Origin version 7.0.

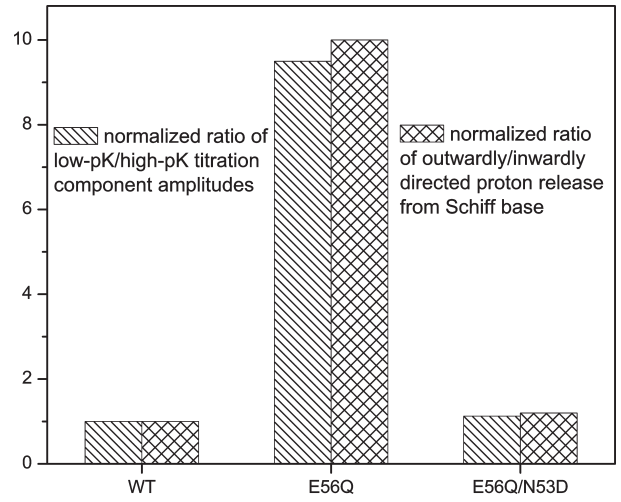

FIGURE 4: Effects of inverting and suppressor mutations on the ratio of amplitudes of the two titration components compared to the ratio of outwardly and inwardly directed Schiff base deprotonation in *E. coli* membranes in a low-ionic strength medium.

of the complexes under high-salt conditions. Two components of the counterion titration are present in this system in the wild-type as well as in the mutated SRI−HtrI complexes (Figure 2, bottom). A remarkable result is that the absolute pK_a values of the two components are not significantly affected by the mutation (7.9 and 9.0 for the wild type and 7.7 and 8.7 for the mutant, respectively), whereas their relative amplitudes change 7.3-fold (Figure 3, left panels). Our interpretation is that the inverting mutation shifts the population of SRI−HtrI complex molecules from the high-pK_a conformer to the low-pK_a conformer.

The large increase in the ratio of the low-pK_a to high-pK_a components caused by the inverting mutation matches closely the changes in the relative size of the pools of outwardly and inwardly connected Schiff bases found earlier by charge movement measurements (*9*). Because these measurements were performed at low ionic strengths, for comparison we performed the pH titration of the wild-type and mutated complexes expressed in *E. coli* membranes also under low-salt conditions (0.1 M NaCl). Results similar to those at 4 M NaCl were obtained: the inverting mutation changes the relative sizes of the low-pK_a and high-pK_a amplitudes in the same direction as at high salt without significant changes in these pK_a values (Figure 3, middle panels). Finally, the effect of the inverting mutation on the relative amounts of low- and high-pK_a conformers in *E. coli* membranes was confirmed to exist in the natural halobacterial membranes (Figure 3, right panels).

Figure 4 illustrates the nearly perfect quantitative correlation of the effects of inverting and suppressor mutations on the ratio of titration components and on the relative fractions of SRI−HtrI complexes with inwardly and outwardly accessible Schiff bases. The inverting (repellent) mutation in transducer HtrI_E56Q increases both ratios by 1 order of magnitude in *E. coli* membranes. The second-site suppressor mutation (HtrI_E56Q_N53D), which restores wild-type attractant signaling, restores nearly completely both parameters.

Both components of pH-induced spectral changes reflect the protonation state of the Schiff base counterion Asp76, since the spectral shift is typical of counterion protonation in SRI and other microbial rhodopsins (*13*−*15*), and no pH dependence of the main absorption maximum was observed when Asp76 was mutated to neutral asparagine (data not shown). In summary, we conclude that the conformer with a low Asp76 pK_a has an outwardly accessible Schiff base and when photoactivated initiates a repellent response, whereas the conformer with the opposite connectivity of the Schiff base has the higher Asp76 pK_a and mediates an attractant response.

The Absorption Spectrum of the Repellent Receptor Conformer Is Blue-Shifted from That of the Attractant Receptor Conformer. The absorption spectra of the wild-type SRI−HtrI complex and the SRI−HtrI_E56Q complex are identical when the Asp76 counterion is neutralized by acidic pH (Figure 5A) or by the D76N mutation (Figure 5B). On the other hand, when Asp76 is ionized the pH shift-induced differential absorption spectra in the range of low pK_a are blue-shifted compared to those in the range of high pK_a (Figure 5C). Hence, the absorption spectrum of the outwardly connected Schiff base (repellent receptor) conformer is blue-shifted compared to that of the inwardly connected (attractant) conformer. The bluer absorption of the low-pK_a conformer with ionized Asp76 is expected from a stronger interaction of Asp76 with the protonated Schiff base (*16*).

Kinase-Activating Activity of Dark-Adapted Attractant and Repellent Receptor Conformers. The frequency of spontaneous swimming reversals in *H. salinarum* cells reflects the activity of the histidinyl kinase CheA (*17*, *18*). In wild-type cells under natural conditions, alterations of the kinase activity following an increase in light intensity are transient, and the steady-state swimming reversal frequency is the same in the dark and in the light (*19*). This homeostasis is accomplished by adaptation machinery in the cells that counteracts the effects of light intensity changes and, at the low natural wild-type SR−Htr complex concentrations, resets the kinase activity, and consequently the swimming reversal frequency, to its prestimulus value (*1*). However, when the receptor−transducer complexes are overexpressed in the cells to >10-fold levels, the adaptation system is not sufficient to reset the kinase activation level (*6*, *20*, *21*)

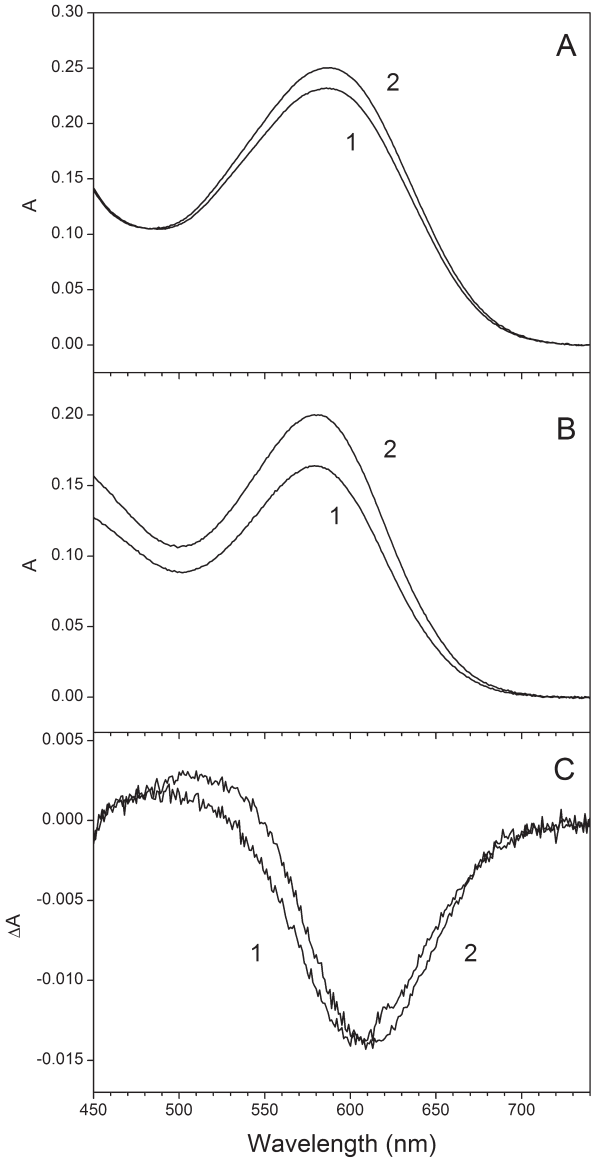

FIGURE 5: (A) Absorption spectra of the wild-type SRI−HtrI complex (1) and the inverted mutant SRI−HtrI_E56Q complex (2) at pH 6.0 in *H. salinarum* membranes. (B) Absorption spectra of the SRI_D76N−HtrI complex with a wild-type behavioral phenotype (1) and inverted mutant SRI_D76N−HtrI_E56Q complex (2) in *E. coli* membranes. (C) pH shift-induced absorption difference spectra of the SRI−HtrI complex in the range of lower pK_a (pH shift from 6.0 to 8.0) (1) and higher pK_a (pH shift from 8.1 to 9.5) (2) in *H. salinarum* membranes.

(J. Sasaki and J. L. Spudich, manuscript in preparation). This effect allows us to compare the kinase-activating activity of different complexes under constant conditions, specifically here in the dark.

Signal-inverting mutations such as E56Q shift the equilibrium of the two conformers in favor of the outwardly accessible Schiff base form (the repellent receptor conformer). The spontaneous swimming reversal frequency in the dark (i.e., dark kinase activity) of these mutants is ~10-fold lower as seen for the SRI−HtrI_E56Q complex (Figure 6). Attractant signaling behavior restored to this mutant by the N53D suppressor mutation restores the wild-type ratio of the two conformer pools (Figure 4) and restores the higher kinase activity as shown by the higher dark reversal frequency (Figure 6). Therefore, the repellent receptor outwardly connected conformer exhibits notably less

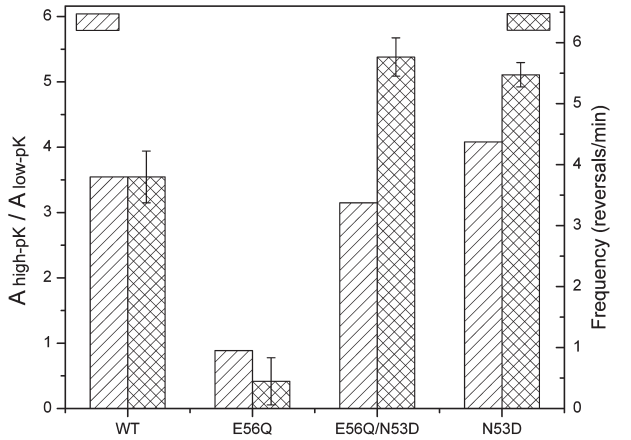

FIGURE 6: Correlation between the relative fraction of the conformer with an inwardly connected Schiff base (left columns) and spontaneous reversal frequency in *H. salinarum* cells overexpressing different SRI−HtrI complexes in the dark (right columns). Error bars indicate the standard deviation of the number of the reversals recorded for 20−30 individual cells.

activation of the kinase than the attractant receptor inwardly connected conformer in the dark. Photostimulation of the outwardly connected form induces swimming reversals (i.e., a repellent response) that indicates its photoproduct activates the kinase, and conversely, photostimulation of the inwardly connected form suppresses swimming reversals (i.e., an attractant response) which indicates its photoproduct inhibits the kinase. These expectations are confirmed by steady-state reversal frequency measurements in the light (J. Sasaki and J. L. Spudich, manuscript in preparation). Note that there is apparently a higher molar efficiency of kinase activation than kinase inhibition from the complex since the overall response is strongly repellent in the presence of close to equal fractions of the two conformers in native membranes (Figure 3, right panels).

A Switch in Schiff Base Connectivity Occurs in the Single-Photon Response of the Wild-Type SRI−HtrI Complex. To test whether the Schiff base switches connectivity after single-photon absorption, we measured the intramolecular charge movement in response to 410 nm laser flashes in the dark-adapted wild-type complex and in the same complex under strong long-wavelength (> 520 nm) background illumination that leads to accumulation of the long-lived unprotonated Schiff base photointermediate M (λ_{max} = 373 nm, also known as S_{373}) in the SRI photocycle (Figure 7). In darkness, only a very small signal with kinetics typical of the photoconversion of the attractant receptor conformer from the dark-adapted SRI−HtrI complex (λ_{max} = 587 nm) was observed, which we attribute to the weak absorption of SRI at 410 nm. Intense orange background illumination converts the dark-adapted form to the M intermediate which absorbs with a λ_{max} of 373 nm and has strong absorption at 410 nm (*1*). The fraction of molecules converted to M was tested by the decrease in the magnitude of the photoelectric signal produced by 580 nm laser flashes (data not shown). Under our condition, 67% of the dark-adapted state is converted. Hence, under orange background illumination, the 410 nm laser-induced electrical signal caused by excitation of the residual nonconverted SRI−HtrI complex should be 33% of the small signal seen without background illumination (Figure 7, curve 1). Therefore, the charge movement elicited by the 410 nm flash in an orange background can be attributed essentially entirely to photoconversion of the M intermediate. The electrical response

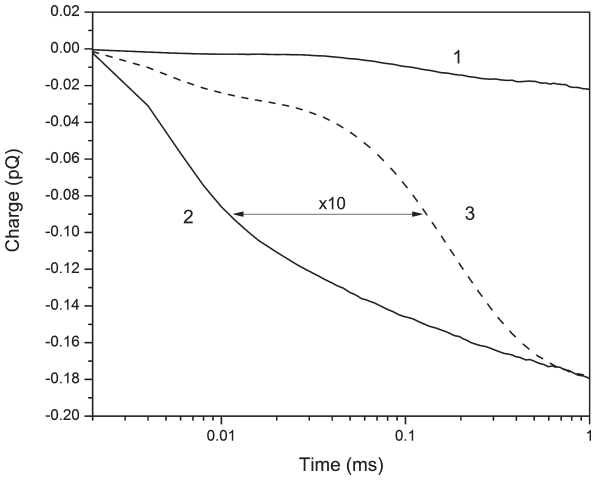

FIGURE 7: Charge movement upon excitation of the short-wavelength intermediate M of the SRI−HtrI complex in *E. coli* membranes. Trace 1 shows the 410 nm laser flash-induced response in darkness. Trace 2 shows the 410 nm laser flash-induced response under continuous orange (> 520 nm) illumination after subtraction of the signal due to the unphotolyzed initial state. Trace 3 shows the normalized signal of the initial state complex in the dark.

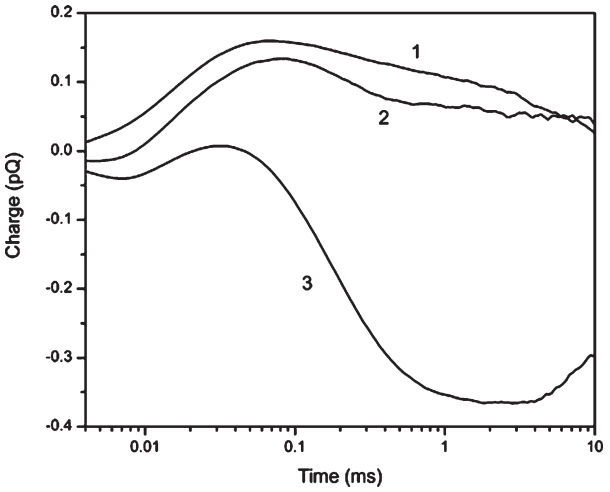

FIGURE 8: Charge movement in the SRII−HtrII complex (1) compared with charge movement in inverted SRI−HtrI_E56Q (2) and wild-type SRI−HtrI (3) complexes in *E. coli* membranes.

of intermediate M photoexcitation is an inwardly directed charge transfer (Figure 7, curve 2), with kinetics > 10-fold faster than those of the inward charge movement from photoexcitation of dark-adapted SRI (Figure 7, curve 3); 410 nm is the shortest output wavelength available from the laser used, and a large decrease in the amplitude of the signal at longer wavelengths, which disappears at 430 nm, corresponds perfectly to the absorption spectrum of SRI M (data not shown).

Photoexcitation of SRI M causes rapid reprotonation of the Schiff base beginning with submicrosecond times (*22*). As shown in curve 2 of Figure 7, this reprotonation causes inwardly directed charge transfer, which therefore must be from the extracellular side (likely from the protonated Asp76). We conclude that SRI M before the absorption of the second short-wavelength photon is in the conformation with the outwardly connected Schiff base. The accelerated inwardly directed charge movement from light-induced Schiff base reprotonation of M as compared to that of the inwardly directed Schiff base deprotonation in dark SRI is in agreement with previously measured kinetics of these processes (*22*).

In conclusion, single photon excitation of the SRI−HtrI attractant conformer causes a Schiff base connectivity switch from the inwardly connected kinase-activating conformation to the outwardly connected kinase-inhibiting conformation. A second near-UV photon drives SRI M back to the unphotolyzed form (*4*) which we show here consists primarily of the inwardly connected conformer. Therefore, we conclude that the inverse connectivity switch from outward to inward occurs when SRI M photoexcitation produces a repellent response.

The Repellent Conformer of the SRI−HtrI Complex Is the Equivalent of the SRII−HtrII Complex. The rapid kinetics of deprotonation of the Schiff base in the outwardly connected conformer of the SRI−HtrI complex (i.e., the inverted mutant) are very similar to those in the second sensory rhodopsin of haloarchaeal SRII, which, in complex with its transducer HtrII, also mediates repellent responses (*1*) (Figure 8). Our electrical measurement confirms that in the dark-adapted state of the SRII−HtrII complex, as previously shown for the transducer-free SRII (*23*−*25*) and the SRII−HtrII complex (*26*, *27*), the Schiff base is outwardly connected and further shows that the kinetics of charge movement are very similar to those in the inverted mutant of the SRI−HtrI complex (Figure 8).

DISCUSSION

Electrophysiological analysis of laser flash-induced currents recently revealed that the SRI−HtrI complex exists in two conformational states with opposite connectivity of the protonated Schiff base in the photoactive site, which is deprotonated during light-induced formation of the signaling state (*9*). Analysis of behavioral mutants indicated that the two conformers mediate opposite motility responses; specifically, the conformer with the Schiff base connected to the cytoplasmic side of the protein produces attractant signals upon photoactivation (i.e., inhibits the protein kinase bound to HtrI), whereas the conformer connected to the outward side produces repellent signals (i.e., activates the kinase).

In this study, we confirm the existence of two conformer pools by different methods not dependent on photoexcitation, namely, absorption spectroscopy and pH titration of dark samples. We found that the pK_a values of the outwardly located Schiff base counterion Asp76 differ in the attractant and repellent receptor conformations of the SRI−HtrI complex, being ~1.5 pH units lower in the latter, as one would expect from the stronger interaction of Asp76 with the Schiff base proton. The pK_a difference enabled assessment of properties of the two conformers not available from photoelectrophysiology, including quantitative determination of the relative amounts of the two conformers in the wild-type and behavioral mutants, assessment of the relative signaling efficiency by the conformers, and measurement of the absorption properties of each conformer.

Two conformers with the oppositely connected Schiff base ensure opposite sides of release and uptake of protons in light-driven ion-pumping rhodopsins (*28*). Our results show that two similar conformers play key roles also in signaling by sensory rhodopsins. The presence of analogous conformers in bacteriorhodopsin's photocycle was likely crucial to the conversion of this proton pump with only three mutations to a robust phototaxis receptor mimicking SRII signaling through HtrII (*29*).

The pH titration of absorption shows that in the wild-type complex ~80% of the molecules are in the inwardly connected attractant receptor conformation. An inverting mutation does

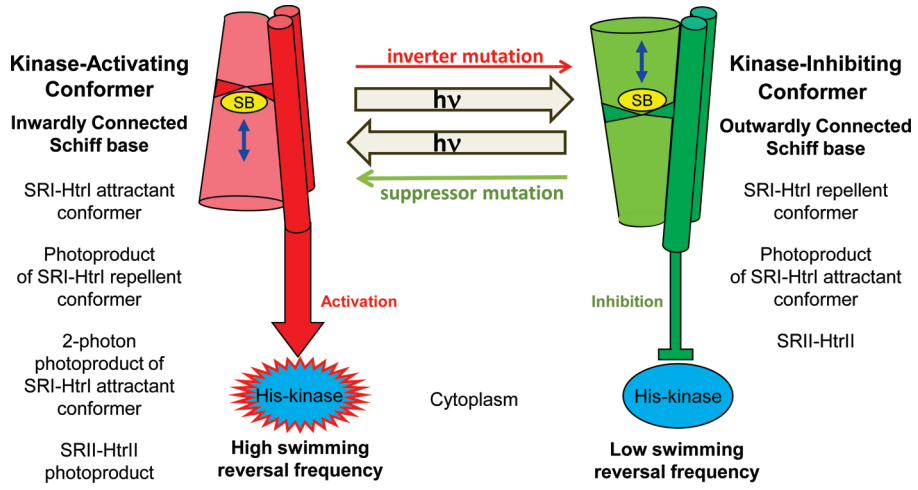

FIGURE 9: Model of the role of Schiff base connectivity switch conformers in dark states and functional intermediates of SR−Htr complexes. By connectivity of the Schiff base we mean the direction, inward or outward, of Schiff base proton release or uptake following photon absorption. Note that by photoproducts in the scheme we mean photointermediates of photocycles that end in initial thermostable conformations.

not change significantly the pK_a values of the attractant and repellent receptor conformers; rather, the relative sizes of the conformer pools is increased 6−10-fold in favor of the repellent conformer with the outwardly connected Schiff base. Suppressor mutations reverse this effect to near the wild-type ratio. The net phototaxis response is strongly repellent in the presence of close to equal fractions of the two conformers in *H. salinarum* cells. Therefore, there appears to be a higher molar efficiency of light-induced kinase activation than kinase inhibition from the complexes. This observation agrees with the finding that in the wild-type cells the second short-wavelength photon not only cancels the attractant effect of the first orange photon but also leads to strong repellent behavior (*4*). Hence, light-induced changes in kinase activity do not reflect merely the shifts in the ratio of pools of the two conformers but involve the different efficiencies and dynamics of downstream elements of signal transduction in the kinase activation and kinase inhibition reactions.

Early studies established that in the wild-type SRI−HtrI complex the long-lived unprotonated Schiff base photointermediate M (λ_{max} = 373 nm, also known as S373) in the SRI photocycle is the attractant signaling state and that it functions as well as a repellent receptor; i.e., its photoactivation by a second photon leads to a repellent response (*1*, *4*, *30*). In view of the results described above, an elegantly simple model results from the generalization of these early findings. Our generalized and more explicit model proposes that interconversions between the same two conformers identified here are responsible for the attractant signal from SRI M accumulation, the repellent response from SRI M photoactivation, the repellent response mediated by inverted mutant SRI−HtrI complexes, and the repellent responses mediated by the SRII−HtrII complex (Figure 9). The essence of the model is that the two conformers are photo-interconvertable; i.e., the photointermediate of the kinase-activating inwardly connected conformer is the kinase-inhibiting outwardly connected conformer, which would produce a decrease in kinase activity, i.e., an attractant response. Conversely, the photoproduct of the kinase-inhibiting conformer is the kinase-activating conformer, which produces an increase in kinase activity. A second key feature is that the conformers inhibit or activate the kinase in a manner independent of whether they are photointermediate states, such as SRI M, or thermostable molecules created by mutation (SRI−HtrI vs SRI−HtrI_E56Q) or by evolutionary changes (SRI−HtrI vs SRII−HtrII). It should be emphasized that upon photoexcitation SR−Htr complexes switch their conformations, which can be distinguished by their opposite Schiff base connectivity, in photointermediate states and the photocycles end with the same thermostable conformation. The return of connectivity to that of the initial state is demonstrated by the observation that the direction of proton movement caused by a second flash after the reappearance of the unphotolyzed spectral state is the same as in response to the first flash.

The switch in Schiff base connectivity from inward to outward in the one-photon attractant signaling photoreaction of the wild-type SRI−HtrI complex reported here is a crucial aspect of the model. Note that this conformational change is the reverse of that occurring in the well-studied bacteriorhodopsin photocycle in which the switch is from outward to inward (*28*). The structural basis of the Schiff base connectivity switch and its coupling to the global conformation of transport rhodopsins has been a subject of great interest, and several models and views have been proposed (reviewed in refs *10*, *31*, and *32*). An atomic-level understanding of this phenomenon is of additional interest given its importance also in sensory rhodopsins. Note that following the finding that HtrI-free SRI carries out light-driven proton transport (*33*) several authors raised the possibility that the conformational changes of transport rhodopsins are involved in sensory rhodopsin signaling (*34*−*37*). Our characterizations of the properties of the signaling conformers here and in our previous study (*9*) confirm that involvement and further show that specifically the Schiff base connectivity switch, the process that ensures vectoriality to the transporters, plays a key role in sensory rhodopsin function.

We emphasize that the connectivity switch is a measurable aspect of a macroconformational transition of a domain of the SR−Htr complex that behaves as a single unit undergoing a concerted transition between two states. Characterization of SRI−HtrI mutants indicates this domain includes the SR photoactive site as well as the membrane portion and membrane-proximal (HAMP) domain of the Htr transducer (*5*, *9*). Evidence of such tight coupling within the complex is the fact that mutations in the transducer subunit of the complex cause long-distance effects in the receptor subunit's photoactive site (*9*). Whether the connectivity switch is a necessary component or

merely an indicator of the photoinduced transition is not yet known.

It is known that a steric conflict with the isomerizing retinal that requires a Thr-Tyr hydrogen-bonded pair in the photoactive site (*38*), a process not observed in transport rhodopsins, is required for signaling by the SRII−HtrII complex (*39*). Introduction of the corresponding Thr-Tyr pair into bacteriorhodopsin by mutation creates the steric conflict (*40*) and converts bacteriorhodopsin into a functional repellent phototaxis receptor (*29*). The relationship of the roles of the steric interaction process and the Schiff base connectivity switch in signaling is not clear and merits further investigation.

One of the most intriguing questions is how the opposite direction of switching between the two conformational states is achieved by the same light input. The absorption spectral maxima of the two conformers differ by 5−10 nm. This difference is eliminated by the Asp76Asn mutation or Asp76 neutralization at low pH and is thereby likely attributable to the difference in counterion charge interaction with the Schiff base proton (*16*). A remarkable finding in this investigation is that in the absence of ionized Asp76, the wild-type and inverted mutant SRI−HtrI complexes, which have greatly different proportions of attractant and repellent conformers, exhibit indistinguishable absorption spectra (Figure 5). Therefore, it is extremely unlikely that the two conformers differ in the isomeric configuration of the retinal around the C13 double bond, which occurs commonly during photocycling of microbial rhodopsins. One possibility is that the inverse direction of light-induced proton release in the two conformers is explained by different conformations of retinal around a single bond, which may have opposite orientations of the Schiff base proton but may not result in a significant absorption shift.

ACKNOWLEDGMENT

We thank Sergei Balashov for insightful and valuable discussions.

REFERENCES

1. Hoff, W. D., Jung, K.-H., and Spudich, J. L. (1997) Molecular mechanism of photosignaling by archaeal sensory rhodopsins. *Annu. Rev. Biophys. Biomol. Struct. 26*, 223–258.
2. Klare, J. P., Gordeliy, V. I., Labahn, J., Buldt, G., Steinhoff, H. J., and Engelhard, M. (2004) The archaeal sensory rhodopsin II/transducer complex: A model for transmembrane signal transfer. *FEBS Lett. 564*, 219–224.
3. Sasaki, J., and Spudich, J. L. (2008) Signal transfer in haloarchaeal sensory rhodopsin-transducer complexes. *Photochem. Photobiol. 84*, 863–868.
4. Spudich, J. L., and Bogomolni, R. A. (1984) Mechanism of colour discrimination by a bacterial sensory rhodopsin. *Nature 312*, 509–513.
5. Jung, K.-H., and Spudich, J. L. (1998) Suppressor mutation analysis of the sensory rhodopsin I-transducer complex: Insights into the color-sensing mechanism. *J. Bacteriol. 180*, 2033–2042.
6. Sasaki, J., Phillips, B. J., Chen, X., Van Eps, N., Tsai, A. L., Hubbell, W. L., and Spudich, J. L. (2007) Different dark conformations function in color-sensitive photosignaling by the sensory rhodopsin I-HtrI complex. *Biophys. J. 92*, 4045–4053.
7. Olson, K. D., Zhang, X. N., and Spudich, J. L. (1995) Residue replacements of buried aspartyl and related residues in sensory rhodopsin I: D201N produces inverted phototaxis signals. *Proc. Natl. Acad. Sci. U.S.A. 92*, 3185–3189.
8. Sineshchekov, O. A., and Spudich, J. L. (2004) Light-induced intramolecular charge movements in microbial rhodopsins in intact *E. coli* cells. *Photochem. Photobiol. Sci. 3*, 548–554.
9. Sineshchekov, O. A., Sasaki, J., Phillips, B. J., and Spudich, J. L. (2008) A Schiff base connectivity switch in sensory rhodopsin signaling. *Proc. Natl. Acad. Sci. U.S.A. 105*, 16159–16164.
10. Lanyi, J. K. (2004) Bacteriorhodopsin. *Annu. Rev. Physiol. 66*, 665–688.
11. Chen, X., and Spudich, J. L. (2002) Demonstration of 2:2 stoichiometry in the functional SRI-HtrI signaling complex in *Halobacterium* membranes by gene fusion analysis. *Biochemistry 41*, 3891–3896.
12. Yao, V. J., and Spudich, J. L. (1992) Primary structure of an archaebacterial transducer, a methyl-accepting protein associated with sensory rhodopsin I. *Proc. Natl. Acad. Sci. U.S.A. 89*, 11915–11919.
13. Marti, T., Rosselet, S. J., Otto, H., Heyn, M. P., and Khorana, H. G. (1991) The retinylidene Schiff base counterion in bacteriorhodopsin. *J. Biol. Chem. 266*, 18674–18683.
14. Rath, P., Olson, K. D., Spudich, J. L., and Rothschild, K. J. (1994) The Schiff base counterion of bacteriorhodopsin is protonated in sensory rhodopsin I: Spectroscopic and functional characterization of the mutated proteins D76N and D76A. *Biochemistry 33*, 5600–5606.
15. Zhu, J., Spudich, E. N., Alam, M., and Spudich, J. L. (1997) Effects of substitutions D73E, D73N, D103N and V106M on signaling and pH titration of sensory rhodopsin II. *Photochem. Photobiol. 66*, 788–791.
16. Yan, B., Spudich, J. L., Mazur, P., Vunnam, S., Derguini, F., and Nakanishi, K. (1995) Spectral tuning in bacteriorhodopsin in the absence of counterion and coplanarization effects. *J. Biol. Chem. 270*, 29668–29670.
17. Rudolph, J., and Oesterhelt, D. (1996) Deletion analysis of the che operon in the archaeon *Halobacterium salinarium*. *J. Mol. Biol. 258*, 548–554.
18. Trivedi, V. D., and Spudich, J. L. (2003) Photostimulation of a sensory rhodopsin II/HtrII/Tsr fusion chimera activates CheA-autophosphorylation and CheY-phosphotransfer in vitro. *Biochemistry 42*, 13887–13892.
19. Spudich, J. L., and Bogomolni, R. A. (1988) Sensory rhodopsins of halobacteria. *Annu. Rev. Biophys. Biophys. Chem. 17*, 193–215.
20. Spudich, E. N., Zhang, W., Alam, M., and Spudich, J. L. (1997) Constitutive signaling by the phototaxis receptor sensory rhodopsin II from disruption of its protonated Schiff base-Asp73 intrahelical salt bridge. *Proc. Natl. Acad. Sci. U.S.A. 94*, 4960–4965.
21. Sasaki, J., Nara, T., Spudich, E. N., and Spudich, J. L. (2007) Constitutive activity in chimeras and deletions localize sensory rhodopsin II/HtrII signal relay to the membrane-inserted domain. *Mol. Microbiol. 66*, 1321–3130.
22. Swartz, T. E., Szundi, I., Spudich, J. L., and Bogomolni, R. A. (2000) New photointermediates in the two photon signaling pathway of sensory rhodopsin-I. *Biochemistry 39*, 15101–15109.
23. Engelhard, M., Scharf, B., and Siebert, F. (1996) Protonation changes during the photocycle of sensory rhodopsin II from *Natronobacterium pharaonis*. *FEBS Lett. 395*, 195–198.
24. Bergo, V., Spudich, E. N., Scott, K. L., Spudich, J. L., and Rothschild, K. J. (2000) FTIR analysis of the SII540 intermediate of sensory rhodopsin II: Asp73 is the Schiff base proton acceptor. *Biochemistry 39*, 2823–2830.
25. Furutani, Y., Iwamoto, M., Shimono, K., Kamo, N., and Kandori, H. (2002) FTIR spectroscopy of the M photointermediate in *pharaonis* rhoborhodopsin. *Biophys. J. 83*, 3482–3489.
26. Bergo, V., Spudich, E. N., Spudich, J. L., and Rothschild, K. J. (2003) Conformational changes detected in a sensory rhodopsin II-transducer complex. *J. Biol. Chem. 278*, 36556–36562.
27. Furutani, Y., Kamada, K., Sudo, Y., Shimono, K., Kamo, N., and Kandori, H. (2005) Structural changes of the complex between *pharaonis* phoborhodopsin and its cognate transducer upon formation of the M photointermediate. *Biochemistry 44*, 2909–2915.
28. Lanyi, J. K. (1995) Bacteriorhodopsin as a model for proton pumps. *Nature 375*, 461–463.
29. Sudo, Y., and Spudich, J. L. (2006) Three strategically placed hydrogen-bonding residues convert a proton pump into a sensory receptor. *Proc. Natl. Acad. Sci. U.S.A. 103*, 16129–16134.
30. Yan, B., and Spudich, J. L. (1991) Evidence that the repellent receptor form of sensory rhodopsin I is an attractant signaling state. *Photochem. Photobiol. 54*, 1023–1026.
31. Herzfeld, J., and Tounge, B. (2000) NMR probes of vectoriality in the proton-motive photocycle of bacteriorhodopsin: Evidence for an 'electrostatic steering' mechanism. *Biochim. Biophys. Acta 1460*, 95–105.
32. Lanyi, J. K., and Luecke, H. (2001) Bacteriorhodopsin. *Curr. Opin. Struct. Biol. 11*, 415–419.
33. Bogomolni, R. A., Stoeckenius, W., Szundi, I., Perozo, E., Olson, K. D., and Spudich, J. L. (1994) Removal of transducer HtrI allows electrogenic proton translocation by sensory rhodopsin I. *Proc. Natl. Acad. Sci. U.S.A. 91*, 10188–10192.

34. Spudich, J. L. (1994) Protein-protein interaction converts a proton pump into a sensory receptor. *Cell 79*, 747–750.
35. Spudich, J. L., and Lanyi, J. K. (1996) Shuttling between two protein conformations: The common mechanism for sensory transduction and ion transport. *Curr. Opin. Cell Biol. 8*, 452–457.
36. Haupts, U., Tittor, J., Bamberg, E., and Oesterhelt, D. (1997) General concept for ion translocation by halobacterial retinal proteins: The isomerization/switch/transfer (IST) model. *Biochemistry 36*, 2–7.
37. Wegener, A. A., Chizhov, I., Engelhard, M., and Steinhoff, H. J. (2000) Time-resolved detection of transient movement of helix F in spin-labelled pharaonis sensory rhodopsin II. *J. Mol. Biol. 301*, 881–891.
38. Sudo, Y., Furutani, Y., Shimono, K., Kamo, N., and Kandori, H. (2003) Hydrogen bonding alteration of Thr-204 in the complex between pharaonis phoborhodopsin and its transducer protein. *Biochemistry 42*, 14166–14172.
39. Sudo, Y., Furutani, Y., Kandori, H., and Spudich, J. L. (2006) Functional importance of the interhelical hydrogen bond between Thr204 and Tyr174 of sensory rhodopsin II and its alteration during the signaling process. *J. Biol. Chem. 281*, 34239–24345.
40. Sudo, Y., Furutani, Y., Spudich, J. L., and Kandori, H. (2007) Early photocycle structural changes in a bacteriorhodopsin mutant engineered to transmit photosensory signals. *J. Biol. Chem. 282*, 15550–15558.